Method and results of the analysis of data on vertical rigidities of cosmic rays cutoff in the geomagnetic field

R.A.Nymmik, M.I.Panasyuk, V.V.Petrukhin, B.Yu.Yushkov
Skobeltsyn Institute of Nuclear Physics, Lomonosov Moscow State University, Moscow, 119991, Russia
nymmik@srd.sinp.msu.ru

ICRC'07 Mérida, México

1 Introduction

The effective cutoff rigidity (ECR) is an important parameter, that characterizes the given point of the near-Earth space, and defines the fluxes at this point as both galactic cosmic rays, and solar energetic particles (SEP) generated during solar flares. These fluxes, along with trapped particles of the Earth's radiation belt, determine the radiation situation onboard the spacecraft. In addition, the geomagnetic cutoff effect allows one to study SEP spectra and fluxes using the data from both neutron monitors (NM), and spacecraft situated inside the magnetosphere.

In practice, the vertical ECR is usually applied (EVCR), which represents a fine estimate averaged over the total ECR body angle [1]. The ECR calculations are based on numerical integration of the equations of motion of charged particles in the geomagnetic field described by any model. Till now, the ECRs were calculated by this technique both for the points of the global NM network, and for many typical orbits of spacecraft, the International Space Station for instance [2, 3]. Note that the ECR depends both on geomagnetic disturbance level, and on the local time [4]. The possibilities of direct ECR calculation permanently grow due to growing power of computers; however, some practical tasks require simpler and less labor-consuming ECR calculation techniques, such as interpolation ones. So, Smart et al have calculated a set of EVCR tables for various conditions and developed the tools for interpolation [5].

2 Proposed EVCR determination technique

The approach we propose is based on interpolation of a basic set of EVCRs calculated with using a series of physical concepts and computational models. The changes of the EVCR value under an effect of magnetosphere disturbance (described by K_p-index) and local time (T) using the Tsyganenko's-89 geomagnetic model [6] are used in the given technique as corrections, whose values are described by the attenuation factor Δ, determined in [7] as:

$$\Delta(R_0, K_p, T) = \frac{R_0}{R(R_0, K_p, T)} - 1 \qquad (1)$$

where R_0 is the initial rigidity calculated for the IGFR model. The reverse conclusion follows from this statement, namely: if the value $\Delta(R_0, K_p, T)$ is known for the given point, then the real EVCR can be determined by the same formula.

The analysis of the results of particles trajectory calculations, carried out according to Tsyganenko's magnetosphere model, leads to the conclusion that the attenuation factor can be presented as two multipliers:

$$\Delta(R_0, K_p, T) = \Delta_1(R_0, K_p) \cdot \Delta_2(R_0, K_p, T) \quad (2)$$

Here Δ_1 is the mean value of the attenuation factor, which does not depend on the local time (T):

$$\Delta_1 = 0.174 \cdot R_0^{-\gamma} \cdot \exp(0.304 \cdot K_p) \qquad (3)$$

where $\gamma = 1.7$ at $R_0 \geq 1\ GV$ and $\gamma = 1.7 \cdot R_0^{-0.1}$ at $R_0 < 1\ GV$. Figure 1 presents the calculated values of the correction quantity Δ_1, which are well described by formula (3). The second multiplier describes the time dependence of EVCR on the mean value of rigidity, K_p-index, and on the local time T:

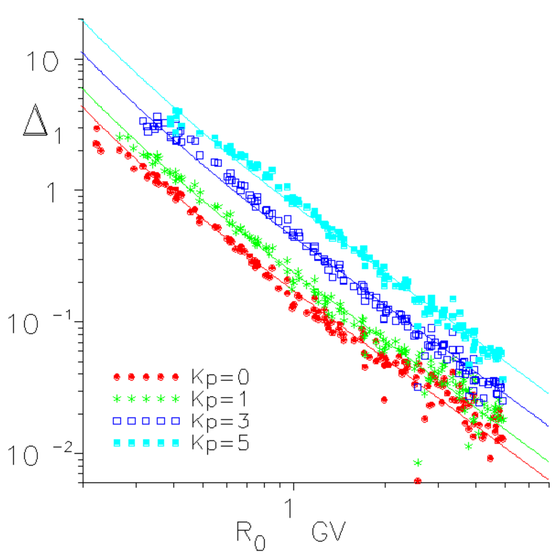

Figure 1: The values of factors of attenuation of EVCR in terms of initial rigidity of IGRF and magnetosphere disturbance levels (from below upwards: $K_p = 0, 1, 3, 5$). Calculated points and their approximations.

$$\Delta_2(R_0, K_p, T) = [1 + A \cdot B \cdot C] \qquad (4)$$

where $A = (0.025 + 0.0344 \cdot K_p)$, $B = R_0^{-(2.42 - 0.075 \cdot K_p)}$ and $C = \sin(\frac{2\pi}{24}(T + \Delta T))$ and where ΔT for the range of rigidities $R = 0.2 \div 0.6\ GV$ has the value of 2 hours approximately.

Formulas (3) and (4) are applicable for determining EVCR for

$$R_0 \geq R_{crit} = 0.238 + 0.029 \cdot K_p \qquad (5)$$

At smaller rigidities, the zero rigidities appear in the evening-night sector - during these periods the given point becomes accessible for penetrating of particles with rigidities smaller than the initial value of the rigidity range looked through, that is equal to 0.001 GV and model becomes incorrect. Figure 2 demonstates an example of the dependences of R and corresponding Δ on LT for such case.

Formulas (1-5) determine the EVCR value for any point of the near-Earth spacecraft's orbit as a function of coordinates, magnetosphere disturbance level and local time value. The use of these formulas allows one to avoid the necessity of performing resource-consuming trajectory calculations of charged particles in the magnetosphere. The validity of this model is confirmed by the results of our numerical calculation of trajectories of charged particles in the geomagnetic field described by the superposition of the IGRF and Tsyganenko-89 models. One of difficulties of such calculations is the verification of numerical integration results. In addition to standard techniques of checking the accuracy control, we have compared our calculations at fixed points with the Smart's et al data [2, 3]. So, we convinced in well coincidence of $R > 0.5\ GV$. The certain distinction lies in the fact, that, with the purpose of increasing the accuracy, in determining the penumbra parameters we have used both the more detailed scale of rigidities - $\Delta R = 0.003\ GV$ (and $\Delta R = 0.001\ GV$ in separate cases), and the algorithm of the fifth order of accuracy [8] for trajectory integration with accounting for the time dependence of the geomagnetic field.

Our calculations of EVCR for the epoch 2005 for the IGRF model are presented in Table 1. Due to calculation's perfomance limits some values in this table with $R < 0.01\ GV$ are not real EVCRs, but their's upper possible values. The EVCR values from Tsyganenko's model for calculating $\Delta_1(R_0, K_p)$ (see Eq. 3) were determined by averaging the data calculated for the set of local time moments $T = 1, 2, \ldots 24$ (hours).

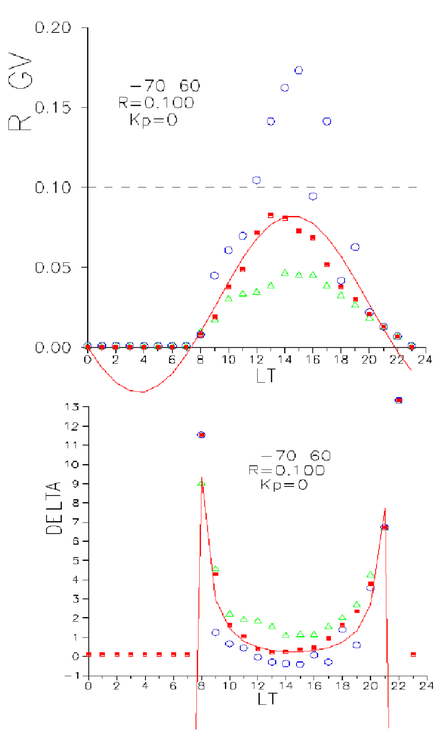

Figure 2: The dependences of Δ and R on LT for the case where extremely low rigitity values are appeared during evening-night local time intervals. R_{up}(blue), R_{bottom}(green), R_{eff}(red) and corresponding Δs.

$\lambda, ^o$	Geographic East Longitude, ^{o}											
	0	30	60	90	120	150	180	210	240	270	300	330
85	0.004	0.004	0.007	0.007	0.010	0.010	0.010	0.013	0.000	0.013	0.007	0.007
80	0.004	0.004	0.004	0.025	0.031	0.016	0.004	0.007	0.010	0.010	0.007	0.004
75	0.040	0.109	0.154	0.178	0.196	0.178	0.127	0.004	0.007	0.007	0.004	0.004
70	0.220	0.316	0.373	0.421	0.454	0.469	0.352	0.169	0.004	0.004	0.004	0.079
65	0.486	0.666	0.741	0.810	0.888	0.951	0.756	0.408	0.144	0.018	0.075	0.282
60	0.990	1.203	1.330	1.426	1.579	1.705	1.408	0.846	0.356	0.174	0.264	0.615
55	1.778	2.018	2.165	2.357	2.588	2.711	2.339	1.460	0.713	0.389	0.560	1.166
50	2.808	3.150	3.351	3.615	3.933	4.101	3.540	2.379	1.262	0.743	1.028	2.010
45	4.223	4.472	4.733	5.084	5.471	5.630	4.739	3.527	2.059	1.285	1.717	3.356
40	6.043	6.244	6.697	7.381	7.850	8.057	6.640	4.768	3.124	1.987	2.641	4.669
35	8.234	8.237	9.098	9.497	9.944	9.635	8.114	6.628	4.387	2.932	3.787	7.063
30	9.766	10.174	10.981	11.663	12.086	11.432	9.955	8.356	5.818	3.789	5.136	9.046
25	11.197	11.779	12.586	13.420	13.324	12.535	11.377	10.057	7.927	5.236	7.006	10.270
20	12.117	12.873	13.678	14.356	14.125	13.209	12.108	11.052	9.153	6.440	8.664	11.208
15	12.634	13.348	14.254	14.950	14.638	13.681	12.673	11.758	10.284	7.683	10.188	11.770
10	12.682	13.480	14.497	15.217	14.875	13.954	13.078	12.280	11.122	9.535	10.840	11.950
5	12.427	13.291	14.413	15.157	14.836	14.017	13.306	12.625	11.731	10.510	11.152	11.851
0	11.908	12.802	14.017	14.770	14.518	13.849	13.339	12.781	12.052	11.113	11.248	11.536
-5	11.140	12.067	13.330	14.062	13.903	13.417	13.147	12.745	12.154	11.335	11.167	11.029
-10	10.231	11.131	12.379	13.027	12.976	12.679	12.691	12.508	12.070	11.356	10.936	10.354
-15	9.111	9.921	10.956	11.500	11.194	11.353	11.935	12.061	11.824	11.188	10.527	9.561
-20	7.718	8.352	9.051	9.381	9.186	9.156	10.374	11.388	11.412	10.890	10.050	8.544
-25	6.337	6.934	7.255	6.634	6.619	7.312	8.392	9.742	10.843	10.450	9.328	7.417
-30	5.262	5.413	5.058	4.635	4.593	5.079	6.682	7.678	10.090	9.829	8.533	6.334
-35	4.246	3.949	3.706	3.100	3.004	3.625	4.798	6.802	8.396	9.134	7.684	5.602
-40	3.436	3.088	2.539	1.933	1.867	2.317	3.541	4.780	6.997	8.234	6.706	4.915
-45	2.777	2.272	1.714	1.165	1.000	1.336	2.275	3.659	5.264	7.218	6.086	3.983
-50	2.229	1.673	1.100	0.611	0.488	0.722	1.424	2.508	3.960	5.440	4.854	3.222
-55	1.718	1.199	0.686	0.294	0.188	0.326	0.806	1.682	2.843	3.924	3.687	2.570
-60	1.297	0.828	0.405	0.111	0.006	0.111	0.405	1.038	1.939	2.851	2.854	1.990
-65	0.948	0.546	0.222	0.000	0.006	0.006	0.195	0.600	1.257	1.866	1.980	1.464
-70	0.640	0.352	0.100	0.004	0.004	0.007	0.046	0.328	0.757	1.163	1.268	0.985
-75	0.415	0.205	0.022	0.004	0.004	0.004	0.004	0.169	0.424	0.664	0.754	0.622
-80	0.229	0.109	0.000	0.004	0.004	0.004	0.004	0.064	0.223	0.347	0.389	0.341
-85	0.106	0.037	0.000	0.004	0.004	0.004	0.004	0.022	0.088	0.139	0.175	0.151

Table 1: Basic EVCR table calculated for IGRF epoch 2005

3 Comparison with experiments and conclusion

We have compared the calculated values of quantity Δ with calculated from EVCR values, obtained by various experiments determined from observations of the boundary of penetration of SEP (protons and alpha-particles). Figure 3 presents the model approximations of attenuation factors for the magneto-quiet conditions, characterized by values $K_p = 0$ and $K_p = 1$. A small arrow stands at the place of critical rigidities R_{crit} (see Eq.5). The set of experimental data is well described by model functions, as a rule.

This model represents the first approximation to the version of the express-calculation technique called for providing a possibility of fast (online) determination of fluxes of particles penetrating to the Earth satellite and orbital stations. In addition, the model is designed for fast determination of the function of particles penetration to projected Earth satellite orbits. This model does not cover the situations, where, along with the magnetosphere disturbance described by the K_p-index, the ring current, described by the D_{st}-index, is simultaneously strengthened in the magnetosphere. In our opinion, such extreme situations occur rather rarely and can be neglected in the first approximation. Besides, some parts of the model need updating.

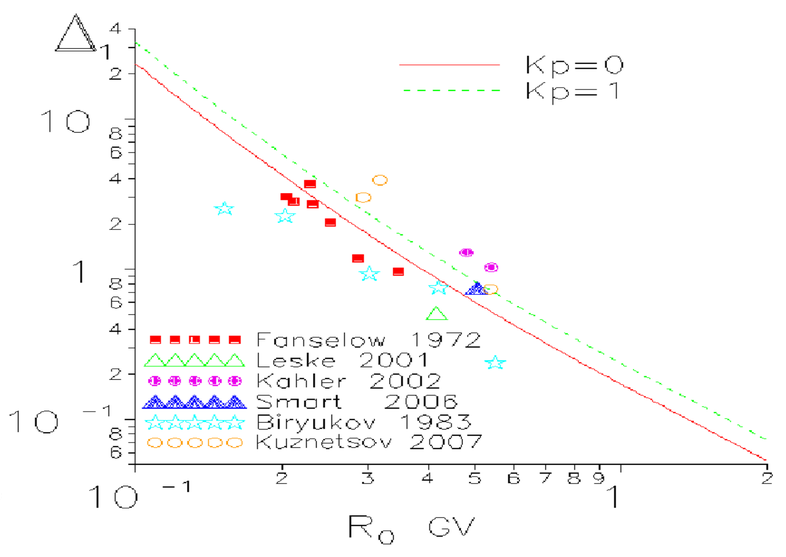

Figure 3: Model dependencies of the time averaged $\Delta(R_{IGRF})$ for $K_p = 0$ and $K_p = 1$, and the Δ_1 values calculated from the results of experiments on near-Earth satellites. The sources of information [9, 10, 11, 12, 13] are deciphered by the first author's name.

References

[1] Smart D.F. et al. Magnetospheric models and trajectory computations. *Space Sci. Rev.*, 93:305–333, 2000.

[2] Smart D.F. et al. Calculated vertical cutoff rigidities for the International Space Station during magnetically quiet times. In *Proc. 26th ICRC*, volume 7 (SH 3.6.28), 1999.

[3] Smart D.F. et al. Calculated vertical cutoff rigidities for International Space Station during magnetically active times. In *Proc. 26th ICRC*, volume 7 (SH 3.6.29), 1999.

[4] Smart D.F. et al. The daily variations of trajectory-derived high-energy latitude cutoff rigidities in a model magnetosphere. *J. Geophys. Res.*, 74:4731–4738, 1969.

[5] Smart D.F. et al. A geomagnetic cutoff rigidity interpolation tool: Accuracy verification and application to space weather. *Advances in Space Research*, 37:1206–1217, 2006.

[6] Tsyganenko N.A. Quantitative models of the magnetospheric magnetic field: methods and results. *Space Sci. Rev.*, 54:75, 1990.

[7] Nymmik R.A. Diurnal variations of geomagnetic cutoff boundaries and the penetration function. *Kosmicheskie issledovaniya (Space Research)*, 29(3):491–493, 1991.

[8] *Nystroem algorithm, procedure 25.5.20.* Handbook Nat. Bur. of Standards.

[9] Fanselow J.L. et al. Geomagnetic cutoffs for Cosmic-Ray protons for seven energy intervals between 1.2 and 39 MeV. *J. Geophys. Res.*, 27(22):3999–4009, 1972.

[10] Leske R.A. et al. Observations of geomagnetic cutoff variations during solar energetic particle events and implications for the radiation environment at the Space Station. *J. Geophys. Res.*, 106(A12):30011–30022, 2001.

[11] Biryukov A.S. et al. Boundary of solar cosmic ray penetration into the magnetosphere in quiet magnitosphere periods. *Kosmicheskie issledovaniya (Space Research)*, 21(6):897–906, 1983.

[12] Kuznetsov S.N. et al. Dynamics of solar energetic particle penetration boundaries into the Earth magnetosphere: CORONAS-F data. *Solar System Research*, 2007, in press.

[13] Kahler S. et al. Comparisons of high latitude $E > 20\ MeV$ proton geomagnetic cutoff observations with predictions of the SEPTR model. *Annales Geophysicae*, 20:997–1005, 2002.